Stochasticity and traffic jams in the transcription of ribosomal RNA: Intriguing role of termination and antitermination

Stefan Klumpp[1] and Terence Hwa

Center for Theoretical Biological Physics and Department of Physics, University of California at San Diego, La Jolla, CA 92093-0374

Edited by David R. Nelson, Harvard University, Cambridge, MA, and approved September 29, 2008 (received for review June 24, 2008)

In fast-growing bacteria, ribosomal RNA (rRNA) is required to be transcribed at very high rates to sustain the high cellular demand on ribosome synthesis. This results in dense traffic of RNA polymerases (RNAP). We developed a stochastic model, integrating results of single-molecule and quantitative in vivo studies of *Escherichia coli*, to evaluate the quantitative effect of pausing, termination, and antitermination (AT) on rRNA transcription. Our calculations reveal that in dense RNAP traffic, spontaneous pausing of RNAP can lead to severe "traffic jams," as manifested in the broad distribution of inter-RNAP distances and can be a major factor limiting transcription and hence growth. Our results suggest the suppression of these pauses by the ribosomal AT complex to be essential at fast growth. Moreover, unsuppressed pausing by even a few nonantiterminated RNAPs can already reduce transcription drastically under dense traffic. However, the termination factor Rho can remove the nonantiterminated RNAPs and restore fast transcription. The results thus suggest an intriguing role by Rho to enhance rather than attenuate rRNA transcription.

Rho-dependent termination | RNA polymerase | transcriptional pausing | elongation-limited transcription | fast bacterial growth

The *rrn* operons encoding ribosomal RNA (rRNA) in fast-growing bacteria are among the most highly transcribed genes known. Fast growth requires a high rate of protein synthesis, which is achieved by a high ribosome concentration in the cell (1). *Escherichia coli* cells, which grow with a doubling time of 20 min, for example, have on average ≈73,000 ribosomes per cell (2, 3). To maintain this high ribosome concentration against fast dilution due to cell growth, rRNA has to be synthesized at very high rates, which are achieved by a combination of large copy number of the *rrn* operons and a high transcription rate per operon. The latter is estimated to be 68 transcripts per minute at a growth rate of 20 min per doubling (3). For comparison, genes encoding mRNA are typically transcribed at rates of 1–10 per minute (4, 5).

As a consequence of their very high transcription rates, the *rrn* operons exhibit a very high density of transcribing RNA polymerases (RNAPs) as visualized by electron microscopy (6). Despite possible "traffic jams" at high densities, RNAPs transcribe rRNA with high elongation speed of 80–90 nt/s (7–10), substantially higher than the elongation speed of 35–55 nt/s known for typical mRNAs (9–11). The higher elongation speed for rRNA transcription was shown to depend on the association of the RNAP with a special antitermination (AT) complex (10), which consists of the Nus proteins, several ribosomal proteins, and a loading sequence (box A) located at the beginning of the rRNA transcript and repeated in the spacer region between the genes encoding the 16S and 23S rRNA (12, 13), see Fig. 1*A*. The higher elongation speed is attributed to the suppression of RNAP pausing (12), which occurs rather frequently, at least in vitro, as revealed by both bulk (14) and single-molecule (15–18) experiments. The physiological implication of the high elongation speed is, however, not clear.* Although one may speculate about a connection between the high speed and the high transcription rate, we note that the transcription rate is usually thought to be controlled by the rate of transcript initiation and the speed of elongation is not considered to have an effect on the transcription rate.

The AT complex suppresses premature termination by the termination factor Rho (12, 20, 21), which binds to the transcript at specific *rut* sites, translocates along it and stops transcription when reaching the RNAP (19, 22). The location of *rut* sites within the *rrn* operons is not known, but studies of various mutants defective in AT (23–26) suggest that termination occurs predominantly in regions immediately downstream of both box A sequences [see Fig. 1*A* and supporting information (SI) *Text*]. The physiological role of Rho-dependent termination for rRNA transcription is not clear. In the case of mRNA, Rho ensures the coupling of transcription and translation via the "polarity" effect (27), i.e., by terminating untranslated transcripts. This is, however, not applicable to rRNA because it is not translated. On the other hand, it seems unlikely that Rho-dependent termination on *rrn* operons is simply a consequence of an unavoidable weak binding of Rho to some generic untranslated transcript, because termination on the *rrn* operons occurs at rather well-defined locations as mentioned above. Furthermore, unlike other termination–AT systems, which play important regulatory roles (28), termination and AT apparently have no role in regulating the expression of the *rrn* operons (12). Thus, the functional role of Rho-dependent termination (and hence the accompanying need of AT) in rRNA transcription is an open question.

In this study, we developed a stochastic model of transcriptional elongation and applied it to the dense RNAP traffic conditions that dominate the transcription of *rrn* operons at fast growth rates. Our model is based on the quantitative characteristics of transcription in vivo and on the dynamics of individual RNAPs as observed in vitro (15–18). Individual RNAPs are observed to move in an asynchronous fashion by stochastic single-nucleotide steps, interrupted by different types of pauses. In dense traffic, a trailing RNAP is likely to catch up and push on a paused RNAP. In our model, this pushing has no effect for the majority of pauses (i.e., it does not push forward the paused RNAP), in accordance with observations in single-molecule experiments that the majority of pauses are unaffected by force applied to the RNAP (18, 29). This important feature leads to the possibility of "traffic jams" in dense RNAP traffic because a paused RNAP may force multiple trailing RNAPs

Author contributions: S.K. and T.H. designed research; S.K. performed research; and S.K. and T.H. wrote the paper.

The authors declare no conflict of interest.

This article is a PNAS Direct Submission.

[1]To whom correspondence should be addressed at: Center for Theoretical Biological Physics, University of California at San Diego, 9500 Gilman Drive, La Jolla, CA 92093-0374. E-mail: klumpp@ctbp.ucsd.edu.

*Faster elongation could contribute to suppress Rho-dependent transcription termination (discussed below), because Rho is less likely to catch up to a faster RNAP (19); but the speed-up effect appears not to be essential for suppressing termination (see *SI Text* for a discussion).

This article contains supporting information online at www.pnas.org/cgi/content/full/0806084105/DCSupplemental.

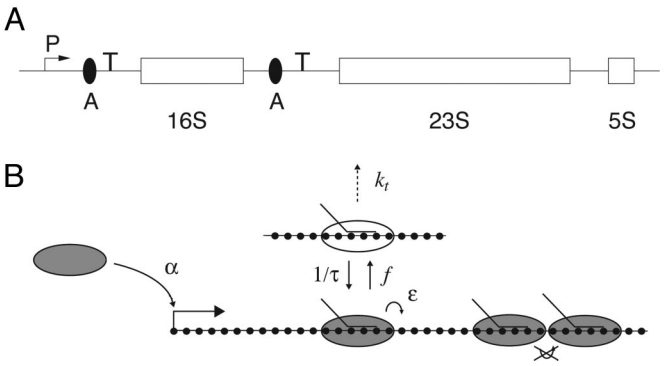

Fig. 1. Modeling transcription of rRNA: (*A*) Schematic structure of an *rrn* operon with the genes encoding the 16S, 23S, and 5S rRNAs (tRNA genes that are present in some *rrn* operons are not shown) showing the loading sequence boxA of the AT complex (black ovals), the approximate positions of rho-dependent terminators as inferred from studies of mutants defective in AT (T) (see *SI Text*), and the promoter pair P1–P2 (P). (*B*) Model for the traffic of RNA polymerases. Active RNAPs (dark gray) elongate an RNA transcript by making single-nucleotide forward steps along the DNA template. These elongation steps occur with rate ε, provided the site in front of the RNAP is not occupied by another RNAP. In addition, RNAPs can switch to an inactive or paused state (white). The transition rate to the paused state is given by the pause frequency f, and a paused RNAP returns to the active state with rate $1/\tau$, where τ is the average pause duration. Paused RNAPs are terminated with rate k_t mimicking Rho-dependent termination. At the promoter (represented by the first site to the left) transcripts are initiated with the initiation attempt rate α if the access of the initiating RNAP to the promoter is not blocked by another RNAP bound there.

to pause as well, hence significantly slowing down the overall rate of transcription.

We used our model to explore systematically the quantitative effect of pausing, termination, and AT on the rate of rRNA transcription. Our results suggest that, indeed, pausing by any individual RNAP during transcription is likely to cause traffic jams that would severely restrict the maximal transcription rate attainable under otherwise optimal conditions for fast growth. In particular, we predict that rRNA could not be transcribed at the high rates necessary to sustain fast growth if the pauses were not suppressed by the AT complex. This theoretical result suggests that AT plays a crucial role for fast growth even in the absence of Rho-dependent termination and that an essential function of the AT complex is antipausing, which is needed to increase the maximal transcription rate.

However, even in the presence of AT, not all RNAPs are antiterminated (30). Therefore, we further studied the effect of pausing by a small fraction of nonantiterminated RNAPs amidst the majority of RNAPs with AT. Our results suggest that the effect of pausing on transcription would be so strong in the dense traffic conditions that rare traffic jams caused by the few nonantiterminated RNAPs could already affect the high rate of rRNA synthesis demanded at rapid growth. We then investigated possible effects of Rho-dependent termination on RNAP traffic and obtained the surprising prediction that higher transcription rates would be attained if Rho could effectively remove the small portion of the stalled, nonantiterminated RNAPs. Our findings suggest an intriguing function for the Rho-dependent termination of rRNA transcription—instead of its commonly understood role in reducing gene expression, Rho may provide a crucial function, under the condition of dense RNAP traffic with a small fraction of nonantiterminated RNAPs, in removing traffic jams and thereby restoring the high transcription rates needed to sustain rapid growth.

Results

To study transcriptional elongation on highly transcribed genes and, in particular, to investigate the effect of RNAP pausing, we developed a stochastic model of RNAP translocation based on in vivo and in vitro data; see *SI Text* for a detailed description. The model is a variant of stochastic cellular automaton models, which have been studied extensively in statistical physics in the contexts of vehicular traffic (31), nonequilibrium phase transitions (32), and cytoskeletal motors (33, 34). Models of this type have also been used extensively to describe the dynamics of ribosomes on mRNA (35–37) and a recent study used a related model (but without pausing or termination) to study the stepping kinetics of RNAP (38). As depicted in Fig. 1*B*, the model allows each RNAP (represented by an oval) to be in the active (dark gray) or the paused (white) states. (An extended version of the model, which also incorporates backtracking, the backward translocation of paused RNAPs, is described in the *SI Text*.) Within the active state, each RNAP may step forward by a single base at the rate ε if the next base is not occupied by another RNAP. We refer to ε as the stepping rate or elongation attempt rate; it gives the maximal instantaneous elongation speed u_0 of a single RNAP, as $u_0 = \varepsilon\, s$ with the step size $s = 1$ nt. The time-averaged elongation speed u of even a single RNAP is smaller than u_0 because of transcriptional pauses. RNAPs are taken to occupy $L = 50$ nt on the DNA template (see *SI Text*). If the first 50 nucleotides are not occupied, a new transcript is initiated with rate α. We call α the "initiation attempt rate;" the actual initiation rate depends on promoter clearance and is in general $<\alpha$.

In the following, we report results from analytical and numerical studies of the above model. We will describe the behavior of this system step by step, first just looking at the effect of RNAP–RNAP interaction, then including the effects of pausing, backtracking, pause suppression by the AT complex, incomplete AT, and finally, termination by Rho. For each case, we used model parameters given in Table 1, which are estimated either directly or indirectly from experimental results as described in *SI Text*. We monitored a number of observable transcriptional characteristics, including the average rate of transcription and elongation and the average density of RNAPs on the transcribed genes and explored the dependence of these results on key model parameters.

Table 1. Model parameters and estimated values

Parameter	Symbol	Value*
Elongation attempt rate	ε	100 s^{-1}
Pause frequency	f	0.1 s^{-1}
Pause duration	τ	1 s
Size of RNAP footprint	L	50 nt
Termination rate	k_t	2–10 s^{-1}

*See *SI Text* for a detailed description of how these values were estimated.

Dense RNAP Traffic Without Pauses. We first considered the case of active transcription only, without pausing or termination. When transcription is infrequent, the average rate of transcription J, i.e., the number of complete transcripts synthesized per minute by 1 operon, is just given by the initiation attempt rate α and is independent of the elongation attempt rate ε. As the transcription frequency increases, the RNAP–RNAP interaction (i.e., mutual exclusion) must be taken into account. Naïvely, one might expect the transcription rate J to be given by α until a critical value $\alpha_c = \varepsilon\, s/L$ set by the clearance rate of the promoter of size L, with J taking on the maximal value $J_{\max} = \alpha_c$ for $\alpha > \alpha_c$ where the RNAPs are closely packed (thin solid lines in Fig. 2*A*). We refer to the regions at small α as the "initiation-limited regime," and the one at large α as the "elongation-limited regime," because they depend only on the initiation and elongation attempt rate, respectively.

However, because of the stochastic, asynchronous nature of RNAP translocation, neighboring RNAPs affect each other's mo-

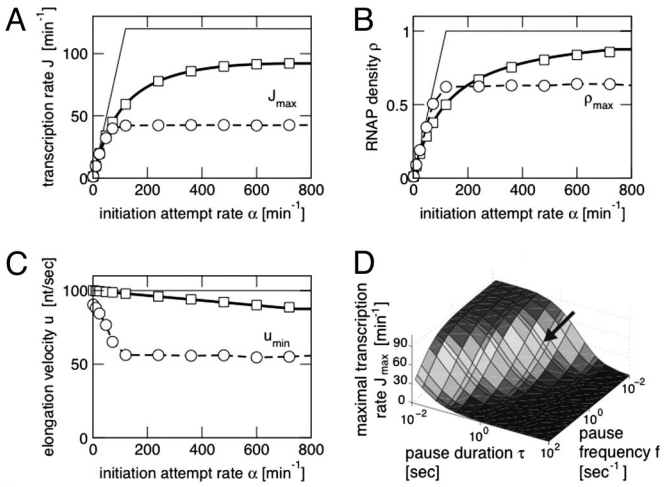

Fig. 2. Effect of pauses during transcription. (*A–C*) Transcription rate J (*A*), RNAP density ρ (*B*), and elongation velocity u (*C*) as functions of the initiation attempt rate α. Thin solid lines indicate the naïve (and incorrect) estimate in which RNAPs move synchronously. Thick solid lines (analytical results as given by Eqs. **1–3** in *SI Text*) and squares (simulations) show results for the case without transcriptional pausing. Circles show the case including pauses with pause parameters from Table 1. (*D*) The maximal transcription rate J_{max}, which is attained for large initiation attempt rates α, as a function of the pause parameters τ and f. The arrow indicates the parameters used in *A–C*.

tion already at densities much below the closely packed limit. This interaction leads to a reduction in the density ρ, the average elongation speed u, and the transcription rate J compared with the naïve expectation. For the case without pauses, exact analytical results of our model are known (35–37); see *SI Text*. These results are plotted as thick solid lines in Fig. 2 *A–C* and have been verified by numerical simulations (symbols). Data over a larger range of α are shown in Fig. S1. Although the average transcription rate J is indistinguishable from the naïve expectation (thin solid line) at very low initiation attempt rate α, it becomes noticeably reduced as α increases. There still exist 2 distinct regimes of α separated by a critical value α_c (marked by the filled triangle in Fig. S1), with J independent of α in the elongation-dominated regime, $\alpha > \alpha_c$.[†] In this regime, the maximal RNAP density is reduced to ≈87% of maximal coverage (compare the thick and thin solid lines in Fig. 2*B*). The average elongation speed, $u(\alpha) = J \cdot L/\rho$, is also diminished for increasing α (Fig. 2*C*), but only by a small amount (≈12% for the minimal speed u_{min}) compared with the maximal elongation speed u_0.

Simulations of our model also allow us to take "snapshots" of the spatial distribution of RNAPs on the operons, similar to the images of transcribed genes taken by electron microscopy (6, 7, 25). From these spatial distributions, we determined histograms of the distance between adjacent RNAPs (Fig. S2). In saturated (elongation-limited) traffic (Fig. S2*A*) the distribution is very narrow, with a strong peak at the minimal possible distance L between RNAPs and a small fraction of longer distances. In dilute traffic (Fig. S2*B*), the distribution is broader, and the maximum of the distribution is at a distance $>L$.

Effect of Transcriptional Pausing. We next investigated the effect of transcriptional pausing, which is modeled as a stochastic process that occurs at a rate f and persists for a period τ, on average; see Fig. 1*B*. According to single-molecule experiments, there are 2 main types of pauses, the "ubiquitous" or "elemental" short pauses and prolonged backtracking pauses (18, 39). In our model, we assume the duration of the short pauses (ubiquitous or elemental pauses) to be independent of the density of RNAP traffic. This assumption is based on the observation that short pauses are unaffected by mechanical force exerted on the RNAP (18, 29), so that a paused RNAP cannot be pushed back into the active state by a trailing RNAP. In contrast, the duration of the less-frequent backtracking pauses, which we study in an extended version of our model in *SI Text*, are found to be significantly shortened in dense traffic (Fig. S3), in agreement with in vitro and in vivo experiments (11). Because the inclusion of backtracking hardly affects the results in the dense traffic regime (Fig. S3), we describe below results for the short pauses only. We also neglect the weak sequence dependence of the short pauses shown by recent single-molecule experiments (17), because it has almost no effect on the results presented here (Fig. S4).

Qualitatively, the results we obtained from simulations including pausing (dashed lines in Fig. 2 *A–C* and Fig. S1) are similar to the case without pausing (thick solid lines). In particular, the 2 different regimes can still be distinguished in the presence of pauses. In the initiation-limited regime ($\alpha < \alpha_c$), the transcription rate J is hardly affected by the pauses at all (Fig. 2*A*). The average elongation speed u is gradually reduced because of pausing (Fig. 2*C*), and the average density ρ is slightly increased (Fig. 2*B*), reflecting the fact that slower RNAPs remain on the operon for a longer time.

On the other hand, the results for the elongation-limited regime ($\alpha > \alpha_c$) depend strongly on the presence of pauses: Pauses with the parameters given in Table 1 reduced the maximal transcription rate J_{max} from 92 min^{-1} to 43 min^{-1} (plateau of the thick lines in Fig. 2*A*, the dependence of J_{max} on the pause parameters is shown in Fig. 2*D*). Similarly, the values ρ_{max} and u_{min} are substantially reduced (Fig. 2 *B* and *C*). In particular, the reduction of the elongation speed is much stronger in dense traffic than in the dilute traffic (40% and 12%, respectively, compared with the case without pauses, see arrows in Fig. S2*C*). This result can be attributed to traffic jams that build up behind paused RNAPs and amplify the effect of pausing (Fig. S5). These traffic jams are also reflected in the histograms of RNAP–RNAP distances (Fig. S2 *C* and *D*), where we observe a strong peak at the minimal distance both in saturated and dilute RNAP traffic.

Effect of Ribosomal AT. As mentioned above, ribosomal RNA operons are transcribed with an elongation speed that is increased approximately 2-fold compared with protein-encoding genes because of the association of the AT complex with the RNAPs transcribing rRNA (10, 40, 41). This increase in speed is generally attributed to the suppression of pauses (see *SI Text* for a discussion). We used our model to see whether the increased elongation speed may be quantitatively explained by only a reduction in the pause duration and what effect this change has on the transcription rate. Our study is predicated on experiments carried out to examine transcriptional characteristics with and without AT in vivo. For example, in the experiments of ref. 10, the elongation speed u of an *rrn* operon was found to be 79 nt/s. This value decreased to 52 nt/s, similar to the elongation speed of mRNA, upon deletion of the AT sequence box*A*. Similar reductions have been observed for various Nus factor mutations (40, 41).

We determined the transcriptional characteristics in the presence and absence of AT, using the measured elongation speeds as sole constraints; see the results as bold entries in Table 2. To do this, we estimated the values of the pause frequency f and the elongation attempt rate ε to be $f = 0.1$ s^{-1} and $\varepsilon = 100$ s^{-1} and took transcription to be in the elongation-limited regime (see *SI Text* and Fig. S6). We further assumed that the pause frequency is unchanged with and without AT as suggested by the related N-dependent AT system (42). We first obtained the value of the pause duration τ with and without AT by demanding the corresponding elongation speeds

[†]In the context of driven diffusive systems, the initiation- and elongation-limited regimes are usually referred to as the low-density phase and the maximal-current phase (32). In addition, the model exhibits a high-density phase, which is not relevant for transcription, because termination of transcription is not limiting the transcription rate.

Table 2. Quantitative effect of antitermination as predicted by the model

Parameter	Without AT	With AT	Fold change
Elongation speed u	52 nt/s	79 nt/s	1.5×
Pause duration τ	**1.17 s**	**0.23 s**	**5×**
Transcription rate J_{max}	**38 min^{-1}**	**76 min^{-1}**	**2×**

The elongation speeds are taken from ref. 10. Data in bold type indicate the predicted transcriptional characteristics at the (predicted) elongation attempt rate of ε = 100/s; see *Effect of Ribosomal AT* in the text for details.

to match those measured in ref. 10, i.e., u_{min} = 79 nt/s with AT and u_{min} = 52 nt/s without AT. The pause duration is found to be τ = 1.17 s in the absence of AT, and 0.23 s in the presence of AT. The result of 1.17 s is in good agreement with the pause duration of ≈1 s observed in single-molecule experiments (15, 17, 18). Also, the predicted reduction in pause duration to 0.23 s (≈5-fold) agrees well with that of the related N-dependent AT system (≈5-fold) as estimated from the data of ref. 42. We further used our model to determine the expected maximal value of the transcription rate, J_{max}, both in the presence and absence of AT. Our simulations predict that AT increases the maximal achievable transcription rate from 38 min^{-1} to 76 min^{-1} (≈2-fold), see Table 2. With this increase, the transcription rate is boosted to the range needed to sustain the fastest growth [68 min^{-1} for 20-min doubling time (3)].

Effect of Partial AT. So far, we have assumed ideal AT assembly and efficiency, i.e., in the presence of the box A sequence each RNAP is antiterminated and exhibits reduced pauses. It has, however, been shown that even in the nominal presence of AT, a fraction of RNAPs is stopped by Rho (30). Experiments with multiple termination sites in sequence further showed that essentially each RNAP that reads through 1 termination site also reads through additional termination further downstream (30). This observation suggests that AT is very effective and rather persistent once an RNAP has become antiterminated but also that not all RNAPs are antiterminated. Partial AT may have a detrimental effect on transcription because RNAPs that are not antiterminated will make longer pauses and may cause jamming even if the majority of RNAPs are antiterminated.

To model the possible consequences of partial AT on *rrn* transcription, we performed simulations for a mixture of RNAPs with and without the AT complex. This is implemented by randomly assigning to each RNAP a pause duration of either 0.2 s (with probability $1 - p$) or 1 s (with probability p) at the initiation of transcription. Here, p indicates the fraction of nonantiterminated RNAPs, and the pause-duration values are chosen according to those in Table 2; they remain unchanged throughout the duration of transcription for each RNAP. In Fig. 3*A*, we show the transcription rate J_{max} obtained from this model for different fractions p of nonantiterminated RNAPs (filled circles). The transcription rate exhibits a rather steep decrease for small percentages of nonantiterminated RNAPs. E.g., if 10% of the RNAPs are not antiterminated, then the maximal transcription rate is predicted to decrease from 81 min^{-1} to 69 min^{-1}, a ≈30% loss of the potential increase in transcription rate due to AT.

Effect of Rho-Dependent Termination. Because the decrease of the transcription rate (filled circles) shown in Fig. 3*A* is caused by the much slower, nonantiterminated RNAPs, we tested the effect of Rho-dependent termination in this context. We performed simulations by incorporating into our model features mimicking forced termination. We only allowed removal of paused nonantiterminated RNAPs.[‡] In one implementation (the "uniform termination model"), we assigned a rate k_t at which any paused nonantiterminated RNAP is removed from the system. In an alternative implementation (the "localized termination model"), we allowed termination (with the same rate k_t) only to occur within the first 1,000 nt of the operon, where RNAPs, on average, pause for the first time, to mimic a termination site located in the leader region of the transcript (Fig. 1*A*).

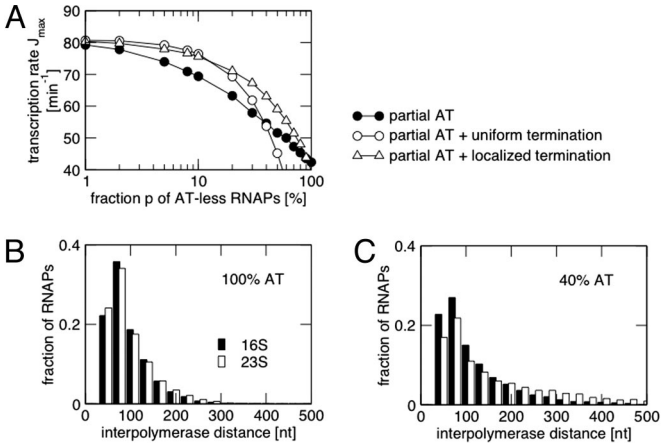

Fig. 3. Effect of partial AT. (*A*) The maximal transcription rate J_{max} as obtained from simulations with 2 populations of RNAPs with different pause durations τ = 0.2 s and τ = 1 s, which represent antiterminated and nonantiterminated RNAPs, respectively (filled symbols). The effect of AT is reduced by the presence of nonantiterminated RNAPs. Termination of the nonantiterminated RNAPs (with a termination efficiency of 80% during pauses, open symbols) can compensate this decrease for small fractions of nonantiterminated RNAPs. (*B* and *C*) Histograms of RNAP-RNAP distances for perfect (*B*) and defective (*C*) AT. Distances between adjacent RNAPs were determined from snapshots of the spatial distribution of RNAPs on simulated *rrn* operons as shown in Fig. 1*A*. Black and white bars show distributions for the 16S and 23S genes, respectively. For perfect AT, the distributions are almost the same; for defective AT, the distribution for the 23S gene is much broader than that for the 16S gene, similar to what has been observed for a NusB mutant (figure 3 in ref. 25).

The simulation results obtained for the 2 models are shown as open symbols in Fig. 3*A*, for a choice of k_t that corresponds to a termination efficiency of 80%, as appropriate for a weak Rho-dependent termination site (30). Similar results are obtained for stronger termination (data not shown). These data show that forced termination increases the maximal transcription rate in both models if the fraction p of nonantiterminated RNAPs is not too large. For the uniform termination model (open circles in Fig. 3*A*), we observe an increase of the transcription rate for p below ≈40% (where the curves with the filled and open circles cross each other). For higher fractions of nonantiterminated RNAPs (and thus also in the complete absence of AT, p = 100%), the transcription rate is, however, found to be strongly reduced, as one would usually expect in the presence of strong indiscriminant termination. For the localized termination model (open squares in Fig. 3*A*), the transcription rate is increased for up to 90% of nonantiterminated RNAPs. Thus, forced termination near the start of transcription initiation can have a substantially more beneficial effect in speeding up transcription. We attribute this effect to the fact that removing nonantiterminated RNAPs soon after initiation not only reduces the number of traffic obstacles but that these nonantiterminated RNAPs are also quite likely to be replaced by antiterminated RNAPs, whereas forced termination downstream of the transcrip-

[‡]The selectivity of rho-dependent termination is higher in our model than in an alternative scenario where selection is only based on the elongation speed (23), see *SI Text* for a discussion.

tion start has the adverse effect of reducing the density of the transcribing RNAP. For both models, the transcription rate can be maintained close to the level of perfect AT with as much as 10% RNAPs without AT. This conclusion remains valid if we consider a more realistic *rrn* operon (Fig. 1*A*) where the AT complex is reloaded in the spacer region between the 16S and 23S genes with an additional termination site immediately downstream (data not shown).

Transcription of rRNA in Wild Type and AT Mutants. Finally we extended our model to the structure of *E. coli rrn* operons as shown in Fig. 1*A*, where the AT complex is assembled in the leader region of the transcript, followed by a termination site, and reassembled in the spacer region between the 16S and 23S genes, again followed by a termination site (see *Methods* in *SI Text* for the modeling details). We used this full version of our model to study the effect of AT mutants. Quan *et al.* (25) have recently characterized viable NusA and NusB mutants. They showed that these strains exhibit polarity between the 16S and 23S genes and quantified this observation using electron microscopy of the *rrn* operons. To see whether our model can account for these observations, we simulated transcription of rRNA with the full model. We chose the initiation attempt rate to be $\alpha = 120\ \text{min}^{-1}$ so that the RNAP density for perfect AT matches the measured density for the wild type (see Table S1, rows 1 and 2). For this value of α, RNAP traffic is dense, ≈73% saturated (data not shown). The transcription rate predicted by our model is $58\ \text{min}^{-1}$ (Table S1, row 2). The transcription rate was not directly measured by Quan *et al.* (25). However, by using the known relation between growth rate and *rrn* transcription for wild-type *E. coli* cells (2, 3), we can predict a corresponding doubling time of ≈24 min, which agrees with the one observed (25). We then varied the degree of AT to mimic defective AT due to NusB or NusA mutations and determined the numbers of RNAPs on the 16S and 23S genes (Table S1), as well as histograms of RNAP–RNAP distances (Fig. 3 *B* and *C*). We obtain quantitative agreement with the experimental values for the number of RNAPs per gene, if we assume 60% of the RNAPs to be not antiterminated in the Nus mutants (Table S1, rows 3–5). We also determined the corresponding transcription rate (of full length transcripts) and estimated the corresponding doubling time to be ≈36–38 min for these mutants (Table S1, row 5). This estimate agrees well with the measured doubling time for the NusA mutant (38 min). The NusB mutant exhibits *rrn* transcription very similar to the NusA mutant but has a substantially larger doubling time of 58 min, possibly indicating an additional defect of this mutant beyond ribosomal AT.

For the wild-type cells and the NusB mutant, Quan *et al.* (25) also determined histograms of the RNAP–RNAP distances measured in electron microscopy images of the *rrn* operons. The corresponding histograms obtained from our model are shown in Fig. 3 *B* and *C*. For perfect AT (Fig. 3*B*), we find that the histograms are almost the same for the 16S and 23S genes, with a strong peak at distances of ≈90 nt and a very small fraction of RNAP–RNAP distances >250 nt, in good agreement with the histograms of ref. 25 for wild-type cells (Table S1). For defective AT with only 40% of the RNAPs antiterminated (Fig. 3*C*), we find that the distribution for the 23S gene is much broader than the one for the 16S gene and that the distributions for both genes are broadened compared with the case of perfect AT with an increased fraction of large distances (Table S1), in good agreement with the results from ref. 25 for the NusB mutant.

Discussion

The rate of transcription is usually thought to be controlled by the rate of transcript initiation, whereas the speed of transcript elongation has no effect on the transcription rate. Although this view is most likely correct for most bacterial genes, we show here that the speed of elongation also plays an important role for highly transcribed genes such as the *rrn* operons in fast-growing bacteria, because it affects the rate of promoter clearance when RNAP traffic is congested. We developed a stochastic model to study such situations, based on the known stochastic dynamics of individual RNAPs (15, 18). In our model, the RNAPs move in an asynchronous fashion, and the pausing of 1 RNAP may impede the stepping of a trailing RNAP. Experimental evidence indicates that backtracked pausing RNAPs may be pushed forward by a trailing RNAP (11). Including this aspect in our model, we find that backtracking pauses should be fully suppressed in dense RNAP traffic (see *SI Text*). However, single-molecule experiments show that the majority of pauses (which are short pauses without backtracking) are unaffected by force applied to the RNAP (18, 29) and thus unlikely to be affected by the pushing force of a trailing RNAP. Our results indicate that the transcription rate can be significantly affected by the stochastic nature of the elongation process, and particularly by transcriptional pausing that creates traffic jams and slows down the overall RNAP traffic (Fig. 2).

Role of AT in rRNA Transcription. RNAPs transcribing rRNA in bacteria are modified by an AT complex that speeds up transcript elongation and suppresses Rho-dependent termination (12, 20, 21, 40).[§] The increase in elongation speed due to AT is attributed to the suppression of transcriptional pausing (12), but the physiological consequence of this antipausing activity is unclear. Our analysis suggest that the suppression of pauses is essential at fast growth where RNAP traffic is dense: The *rrn* operons in fast-growing bacteria are highly transcribed, with transcription rates of up to ≈70 transcripts per minute per operon (2, 3).[¶] According to our analysis, it is not possible to obtain transcription rates of this magnitude in the absence of AT (Table 2), given the known dynamics of elongation with pauses (15, 18) and the speed of transcription measured in vivo in the absence of AT [52 nt/s (10)], because pausing RNAPs in dense traffic induce RNAP traffic jams.[‖] With AT, we find that both the physiologically required transcription rate for fast growth [$68\ \text{min}^{-1}$ at 20-min doubling time (3)] and the observed increase in elongation speed [to 79 nt/s (10)] can be quantitatively explained by a 5-fold decrease in the pause duration from ≈1 s to ≈0.2 s (Table 2). Our results suggest that an essential physiological function of ribosomal AT is antipausing, designed to increase the transcription rate of rRNA to sustain the demand at rapid growth, rather than to suppress Rho-dependent termination. We predict that mutants with defective AT will exhibit growth defects, mainly at very rapid growth, even if Rho-dependent termination is not operative there, e.g., in Rho or *rut* site mutants, or if Rho activity is suppressed by an antibiotic (45). For cells defective in both AT and Rho activity, Table 2 makes quantitative predictions for the transcription rate of rRNA and the doubling time for growth in rich medium. We note however that such experiments are not easy to do or interpret, because ribosome synthesis is a core component of cell growth, and perturbations likely have additional effects.

Role of Rho-Dependent Termination in rRNA Transcription. The above interpretation of *rrn* AT as an antipausing mechanism naturally leads to questions on possible function(s) for Rho-dependent termination in rRNA transcription. Rho-dependent termination ensures the coupling of transcription and translation for protein-

[§]The AT complex is likely to have additional functions such as adapting the elongation speed for optimal folding of rRNA (42), facilitating rRNA processing (44), and assembly of the ribosome subunits (13), which are outside the scope of this study.

[¶]Even higher transcription rates are necessary in strains with reduced numbers of *rrn* operons, see *SI Text* for a discussion.

[‖]The transcription rates without AT are, however, sufficient to account for the transcription of highly transcribed protein-encoding genes such as those encoding ribosomal proteins (5).

encoding genes as evidenced by the polarity effect (27), but its role for rRNA genes has not been addressed previously. Our simulations indicate that the rate of rRNA transcription can be significantly reduced by the presence of even a small fraction (e.g., 10%) of nonantiterminated RNAPs, which make longer pauses (Fig. 3). Because even in the presence of AT, not all RNAPs are antiterminated (30), such nonantiterminated RNAPs are expected to appear in the transcription of rRNA. The high transcription rates needed for fast growth thus require a mechanism to remove these obstacles. We propose that Rho-dependent termination can provide such a mechanism (Fig. 3): Assuming that Rho can efficiently terminate those RNAPs that escaped AT, e.g., removing a large fraction of them during their longer pauses, results of our simulations predict that the reduction in transcription can be almost entirely restored, unless the fraction of nonantiterminated RNAPs is so large that removing them leads to significant reduction in RNAP density. We thus conclude that Rho-dependent termination could actually increase rather than decrease transcription, as one would naïvely expect. In this way, Rho-dependent termination may be recruited to work as an integral part of a transcriptional system designated to achieve high transcription rates for rRNA.

ACKNOWLEDGMENTS. S.K. was supported in part by a fellowship from Deutsche Forschungsgemeinschaft (Grants KL818/1-1 and 1-2). S.K. and T.H. are grateful for further support from the National Science Foundation through Grant PHY-0822283 to the Physics Frontiers Centers-sponsored Center for Theoretical Biological Physics, and for Grant MCB0746581 (to T.H.).

1. Schaechter M, Maaløe O, Kjeldgaard NO (1958) Dependency on medium and temperature of cell size and chemical composition during balanced growth of *Salmonella typhimurium*. *J Gen Microbiol* 19:592–606.
2. Bremer H, Dennis PP (1996) Modulation of chemical composition and other parameters of the cell by growth rate. *Escherichia coli and Salmonella*, ed Neidhardt FC (Am Soc Microbiol, Washington, DC), 2nd Ed, pp1553–1569.
3. Bremer H, Dennis PP (2008) Modulation of chemical composition and other parameters of the cell at different exponential growth rates. *EcoSal-Escherichia coli and Salmonella*, http://www.ecosal.org/ecosal/index.jsp, Module 5.2.3.
4. Bon M, McGowan SJ, Cook PR (2006) Many expressed genes in bacteria and yeast are transcribed only once per cell cycle. *FASEB J* 20:1721–1723.
5. Liang ST, *et al.* (1999) Activities of constitutive promoters in *Escherichia coli*. *J Mol Biol* 292:19–37.
6. Gotta SL, Miller OL, French SL (1991) rRNA transcription rate in *Escherichia coli*. *J Bacteriol* 173:6647–6649.
7. Condon C, French S, Squires C, Squires CL (1993) Depletion of functional ribosomal RNA operons in *Escherichia coli* causes increased expression of the remaining intact copies. *EMBO J* 12:4305–4315.
8. Molin S (1976) Ribosomal RNA chain elongation rates in *Escherichia coli*. *Control of Ribosome Synthesis Alfred Benzon Symposium IX*, eds Kjeldgaard NO, Maaloe O (Munksgaard, Copenhagen), pp 333–341.
9. Vogel U, Jensen KF (1994) The RNA chain elongation rate in *Escherichia coli* depends on the growth rate. *J Bacteriol* 176:2807–2813.
10. Vogel U, Jensen KF (1995) Effects of the antiterminator boxA on transcription elongation kinetics and ppGpp inhibition of transcription elongation in *Escherichia coli*. *J Biol Chem* 270:18335–18340.
11. Epshtein V, Nudler E (2003) Cooperation between RNA polymerase molecules in transcription elongation. *Science* 300:801–805.
12. Condon C, Squires C, Squires CL (1995) Control of rRNA transcription in *Escherichia coli*. *Microbiol Rev* 59:623–645.
13. Torres M, Condon C, Balada JM, Squires C, Squires CL (2001) Ribosomal protein S4 is a transcription factor with properties remarkably similar to NusA, a protein involved in both non-ribosomal and ribosomal RNA antitermination. *EMBO J* 20:3811–3820.
14. Kassavetis GA, Chamberlin MJ (1981) Pausing and termination of transcription within the early region of bacteriophage-T7 DNA in vitro. *J Biol Chem* 256:2777–2786.
15. Adelman K, *et al.* (2002) Single molecule analysis of RNA polymerase elongation reveals uniform kinetic behavior. *Proc Natl Acad Sci USA* 99:13538–13543.
16. Davenport RJ, Wuite GJL, Landick R, Bustamante C (2000) Single-molecule study of transcriptional pausing and arrest by *E-coli* RNA polymerase. *Science* 287:2497–2500.
17. Herbert KM, *et al.* (2006) Sequence-resolved detecton of pausing by single RNA polymerase molecules. *Cell* 125:1083–1094.
18. Neuman KC, Abbondanzieri EA, Landick R, Gelles J, Block SM (2003) Ubiquitous transcriptional pausing is independent of RNA polymerase backtracking. *Cell* 115:437–447.
19. Jin DJ, Burgess RR, Richardson JP, Gross CA (1992) Termination efficiency at rho-dependent terminators depends on kinetic coupling between RNA polymerase and rho. *Proc Natl Acad Sci USA* 89:1453–1457.
20. Aksoy S, Squires CL, Squires C (1984) Evidence for antitermination in *Escherichia coli* rRNA transcription. *J Bacteriol* 159:260–264.
21. Holben WE, Morgan EA (1984) Antitermination of transcription from an *Escherichia coli* ribosomal RNA promoter. *Proc Natl Acad Sci USA* 81:6789–6793.
22. Richardson JP (2002) Rho-dependent termination and ATPases in transcript termination. *Biochim Biophys Acta* 1577:251–260.
23. Heinrich T, Condon C, Pfeiffer T, Hartmann RK (1995) Point mutations in the leader boxA of a plasmid-encoded *Escherichia coli* rrnB operon cause defective antitermination in vivo. *J Bacteriol* 177:3793–3800.
24. Pfeiffer T, Hartmann RK (1997) Role of the spacer boxA of *Escherichia coli* ribosomal RNA operons in efficient 23 S rRNA synthesis in vivo. *J Mol Biol* 265:385–393.
25. Quan S, Zhang N, French S, Squires CL (2005) Transcriptional polarity in rRNA Operons of *Escherichia coli* nusA and nusB mutant strains. *J Bacteriol* 187:1632–1638.
26. Sharrock RA, Gourse RL, Nomura M (1985) Defective antitermination of rRNA transcription and derepression of rRNA and tRNA synthesis in the NusB5 mutant of *Escherichia coli*. *Proc Natl Acad Sci USA* 82:5275–5279.
27. Adhya S, Gottesman M (1978) Control of transcription termination. *Annu Rev Biochem* 47:967–996.
28. Nudler E, Gottesman ME (2002) Transcription termination and anti-termination in *E. coli*. *Genes Cells* 7:755–768.
29. Dalal RV, *et al.* (2006) Pulling on the nascent RNA during transcription does not alter kinetics of elongation or ubiquitous pausing. *Mol Cell* 23:231–239.
30. Albrechtsen B, Squires CL, Li S, Squires C (1990) Antitermination of characterized transcriptional terminators by the *Escherichia coli* rrnG leader region. *J Mol Biol* 213:123–134.
31. Chowdhury D, Santen L, Schadschneider A (2000) Statistical physics of vehicular traffic and some related systems. *Phys Rep* 329:199–329.
32. Schütz GM (2001) Exactly solvable models for many-body systems far from equilibrium. *Phase Transitions and Critical Phenomena*, eds Domb C, Lebowitz JL (Academic, San Diego), Vol 19, pp 1–251.
33. Lipowsky R, Klumpp S, Nieuwenhuizen TM (2001) Random walks of cytoskeletal motors in open and closed compartments. *Phys Rev Lett* 87:108101.
34. Parmeggiani A, Franosch T, Frey E (2003) Phase coexistence in driven one-dimensional transport. *Phys Rev Lett* 90:086601.
35. MacDonald CT, Gibbs JH, Pipkin AC (1968) Kinetics of biopolymerization on nucleic acid templates. *Biopolymers* 6:1–25.
36. Lakatos G, Chou T (2003) Totally asymmetric exclusion processes with particles of arbitrary size. *J Phys A* 36:2027–2041.
37. Shaw LB, Zia RKP, Lee KH (2003) Totally asymmetric exclusion process with extended objects: A model for protein synthesis. *Phys Rev E* 68:021910.
38. Tripathi T, Chowdhury D (2008) Interacting RNA polymerase motors on a DNA track: Effects of traffic congestion and intrinsic noise on RNA synthesis. *Phys Rev E* 77:011921.
39. Landick R (2006) The regulatory roles and mechanism of transcriptional pausing. *Biochem Soc Trans* 34:1062–1066.
40. Vogel U, Jensen KF (1997) NusA is required for ribosomal antitermination and for modulation of the transcription elongation rate of both antiterminated RNA and mRNA. *J Biol Chem* 272:12265–12271.
41. Zellars M, Squires CL (1999) Antiterminator-dependent modulation of transcription elongation rates by NusB and NusG. *Mol Microbiol* 32:1296–1304.
42. Mason SW, Li J, Greenblatt J (1992) Host factor requirements for processive antitermination of transcription and suppression of pausing by the N protein of bacteriophage lambda. *J Biol Chem* 267:19418–19426.
43. Lewicki BTU, Margus T, Remme J, Nierhaus KH (1993) Coupling of rRNA transcription and ribosomal assembly in vivo (1993) *J Mol Biol* 231:581–593.
44. Morgan EA (1986) Antitermination mechanisms in rRNA operons of *Escherichia coli*. *J Bacteriol* 168:1–5.
45. Cardinale CJ, *et al.* (2008) Termination factor Rho and its cofactors NusA and NusG silence foreign DNA in *E. coli*. *Science* 320:935–938.